Numerical Test for Stability Evaluation of Analog Circuits

Tomasz P. Stefański, Piotr Kowalczyk
Faculty of Electronics, Telecommunications and Informatics
Gdansk University of Technology
Gdansk, Poland
Emails: tomasz.stefanski@pg.edu.pl, piotr.kowalczyk@pg.edu.pl

Jacek Gulgowski
Faculty of Mathematics, Physics and Informatics
University of Gdansk
Gdansk, Poland
Email: jacek.gulgowski@ug.edu.pl

***Abstract*—In this contribution, a new numerical test for the stability evaluation of analog circuits is presented. Usually, if an analog circuit is unstable then the roots of its characteristic equation are localized on the right half-plane of the Laplace s-plane. Because this region is unbounded, we employ the bilinear transformation to map it into the unit disc on the complex plane. Hence, the existence of any root inside the unit disc implies circuit instability. In our test, we employ the global roots and poles finding algorithm based on phase analysis to detect the roots of the characteristic equation inside the unit disc. Unlike other stability tests, our approach allows one to evaluate the stability of analog circuits and systems whose characteristic equations are not polynomials. In order to demonstrate its efficiency, generality and applicability, we analyze a memristor-based chaotic circuit whose stability depends on the value of the fractional-order parameter. The proposed test correctly detects the parameter ranges of either stability or instability for the considered analog circuit.**

***Keywords*—Circuit theory, stability analysis, circuit simulation, fractional calculus.**

I. Introduction

Stability is a fundamental property required in the design process of most analog circuits. Therefore, stability evaluation is the topic of numerous chapters in encyclopedias [1] and circuit theory handbooks [2], in addition to being an active topic of scientific publications [3]. Usually, the stability of an analog circuit stems from the lack of roots of its characteristic equation on the right half-plane of the Laplace transform domain (i.e., the Laplace s-plane). It is currently fairly easy to evaluate the circuit stability if its characteristic equation is a polynomial. For this purpose, one can use Hurwitz and Routh criteria [2] or numerical tools for the computations of polynomial roots which are available, e.g., in Matlab [4]. However, there are various nonlinear circuits and systems (e.g., refer to [5], [6]) whose characteristic equations are general, nonlinear complex functions of the complex variable. In this case, one can apply the investigated by us methods for stability evaluation.

In [7], [8], we present general methods for stability evaluation of discrete-time circuits and systems, such as digital filters, employing the global roots and poles finding (GRPF) algorithm based on phase analysis [9]. These methods can be extended with the bilinear transformation in order to allow for evaluating the stability of continuous-time circuits and systems (e.g., analog circuits). This procedure is the main result of this contribution. We hereby propose mapping the instability region into the unit disc on the complex plane and introduce an efficient numerical method for root detection in this region. In order to demonstrate its applicability, we analyze a memristor-based chaotic circuit whose stability depends on the value of the fractional-order (FO) parameter [10]. The proposed test correctly detects the parameter ranges of either stability or instability for the considered analog circuit, proving the efficiency and generality of our stability test.

II. Proposed Stability Test

Let us introduce the stability test applicable to analog circuits and systems, which are described by FO derivatives. This approach yields characteristic equations of the non-polynomial type.

A. Stability Definition

Let us consider the continuous-time autonomous system

$$D_t^q \mathbf{x}(t) = \mathbf{f}\left[\mathbf{x}(t)\right] \qquad \mathbf{x}(0) = \mathbf{x}_0 \tag{1}$$

where $\mathbf{x}(t) \in \mathbb{R}^n$ denotes the state vector, $\mathbf{f} : \mathbb{R}^n \mapsto \mathbb{R}^n$ is the continuously differentiable vector function, $\mathbf{x}(0) = \mathbf{x}_0$ is the initial condition set at $t = 0$, $n \in \mathbb{N}$ and $q \in (0, 1)$. In (1), the FO derivatives of vector elements are defined based on the Caputo definition

$$D_t^\alpha f(t) = J_t^{m-\alpha} D_t^m f(t) \tag{2}$$

where $\alpha \in (m-1, m)$, $m \in \mathbb{N}$, D_t^m is the integer-order derivative, and J_t^α is the Riemann-Liouville integral defined as

$$J_t^\alpha f(t) = \frac{1}{\Gamma(\alpha)} \int_a^t f(\tau)(t-\tau)^{\alpha-1}\,\mathrm{d}\tau. \tag{3}$$

In (3), a is the fixed base point. Although the applications of the Caputo definition in the circuit theory cause serious theoretical difficulties [11], [12], we employ it to maintain consistency with the results of an exemplary circuit analysis [10]. Next, we employ the following property of the Laplace transformation $\mathcal{L}$ for the Caputo derivative:

$$\mathcal{L}\{D_t^\alpha f(t)\} = s^\alpha \mathcal{L}\{f(t)\} - \sum_{k=0}^{m-1} s^{\alpha-k-1} f^{(k)}(0). \tag{4}$$

Remark. The complex power function is, in general, multi-valued. In this investigation, we define it as the single-valued map $s \mapsto s^q$ on the domain $\mathbb{C} \setminus \{x + jy : x \leq 0 \wedge y = 0\}$ by the formula

$$s^\alpha = |s|^\alpha e^{j\alpha \arg(s)} \tag{5}$$

where $\arg(s) \in (-\pi, \pi)$.

Definition II.1. The point $\mathbf{x}_{eq}$ is the equilibrium point of (1) if $\mathbf{f}[\mathbf{x}_{eq}] = \mathbf{0}$, which is equivalent to $D_t^q \mathbf{x}(t) = \mathbf{0}$ at this point.

Remark. The equilibrium point $\mathbf{x}_{eq}$ can be shifted to the origin $\tilde{\mathbf{x}}(t) = \mathbf{0}$ by the substitution $\tilde{\mathbf{x}}(t) = \mathbf{x}(t) - \mathbf{x}_{eq}$. It is further assumed, without loss of generality, that the equilibrium point of the considered system (1) is located in the origin.

One can linearise the system (1) at the equilibrium point $\mathbf{x}_{eq}$. Then one obtains

$$D_t^q \mathbf{x} = \mathbf{J}\mathbf{x} \tag{6}$$

where

$$\mathbf{J} = \left(\frac{\partial \mathbf{f}}{\partial \mathbf{x}} \right)_{\mathbf{x}=\mathbf{x}_{eq}} \tag{7}$$

is the Jacobian matrix.

Definition II.2. The equilibrium point $\mathbf{x}_{eq}$ of the autonomous system (1) is said to be:

- stable iff

$$\forall_{\epsilon>0} \exists_{\delta>0} \forall_{t \geq 0} \quad \|\mathbf{x}_0 - \mathbf{x}_{eq}\| < \delta \implies \|\mathbf{x}(t) - \mathbf{x}_{eq}\| < \epsilon \tag{8}$$

- asymptotically stable iff it is stable and

$$\exists_{\sigma>0} \quad \|\mathbf{x}_0 - \mathbf{x}_{eq}\| < \sigma \implies \lim_{t \to +\infty} \|\mathbf{x}(t) - \mathbf{x}_{eq}\| = 0 \tag{9}$$

- unstable iff it is not stable.

Remark. For the nonlinear function $\mathbf{f}$ in the system (1), the term *locally stable* (or *globally stable*) is often used to underline the local (or global) character of the stability definition.

A theorem can be formulated which relates the local stability of system (1) (i.e., in the neighbourhood of the equilibrium point) to the stability of its linearised counterpart (6).

Theorem II.1. If the equilibrium point $\mathbf{x}_{eq}$ is asymptotically stable for (6), then this point is also *locally* asymptotically stable for (1).

For integer-order systems with $q = 1$, this theorem is the conclusion from the first method of Lyapunov (for continuous-time autonomous systems) [1]. The justification and application of such a stability theorem, formulated for FO systems described with the use of Caputo derivative, can be found in [10], [13], [14].

Remark. The concept of asymptotic stability in Theorem II.1 is *local*, hence the region of asymptotic stability can be large for some systems and very small for others. There is no general method allowing one to determine the limits of this stability region.

Let us transfer (6) into the Laplace domain and provide the conditions for the stability of this system. In the Laplace domain, one can write (6) as follows:

$$s^q \mathbf{x} = \mathbf{J}\mathbf{x} + s^{q-1}\mathbf{x}_0. \tag{10}$$

The characteristic equation of (10) is given by

$$\det(s^q \mathbf{I} - \mathbf{J}) = 0 \tag{11}$$

where $\mathbf{I}$ denotes the identity matrix. Therefore, we can formulate a theorem relating eigenvalues of $\mathbf{J}$ (i.e., spec($\mathbf{J}$)) to the system stability.

Theorem II.2. [15] The system (6) is

- asymptotically stable iff $|\arg(\text{spec}(\mathbf{J}))| > q\pi/2$. In this case, the components of the state vector decay towards zero like t^{-q}
- stable iff either it is asymptotically stable, or the critical eigenvalues which satisfy $|\arg(\text{spec}(\mathbf{J}))| = q\pi/2$ have geometric multiplicity equal to one.

The theorem given above defines the stability region in terms of eigenvalues of the matrix $\mathbf{J}$. Alternatively, one can formulate Theorem II.2 in terms of solutions to the non-polynomial characteristic equation (11). It is expressed in the following way:

Theorem II.3. The system (6) is

- asymptotically stable iff all the roots of the characteristic equation (11) are on the left half-plane of the complex s-plane. In this case, the components of the state vector decay towards zero like t^{-q}
- stable iff either it is asymptotically stable, or those critical solutions on the imaginary axis $\Re s = 0$ correspond to eigenvalues of geometric multiplicity equal to one.

This theorem implies that one can find the roots of the characteristic equation (11) and state that the considered system is unstable if any $(1/q)$-th power of an eigenvalue exists on the right half s-plane. This version of the theorem allows us to work with the complex half-plane rather than a cone (or wedge) given in Theorem II.2, which appears to be a more general approach. That is, it targets all the systems whose roots of the characteristic equation on the right half-plane imply instability.

B. Conformal Mappings

Our aim is to evaluate the stability of analog circuits which are unstable, if any root exists on the right half-plane of the complex s-plane. In order to employ the GRPF algorithm for this purpose, one has to transform the right-hand side of the complex plane into a bounded region. We employ the bilinear transformation

$$s = \frac{1 - w}{1 + w} \tag{12}$$

for this purpose, which is the 1–1 mapping between the open right half-plane and the unit disc $|w| < 1$.

C. GRPF Algorithm

GRPF operates on four complex-plane quadrants ($\{Q_1 : 0 \leq \arg[g(w)] < \pi/2\}$, $\{Q_2 : \pi/2 \leq \arg[g(w)] < \pi\}$, $\{Q_3 : \pi \leq \arg[g(w)] < 3\pi/2\}$, $\{Q_4 : 3\pi/2 \leq \arg[g(w)] < 2\pi\}$), related to the values of the considered function $g(w)$ [9]. Roots of the characteristic equation $g(w) = 0$ are detected based on the unit-disc triangulation (or the triangulation of a rectangular domain containing the unit disc inside), and Cauchy's argument principle [16]. That is, GRPF verifies if any root exists and then locates it with the use of Delaunay's triangulation [17] of the complex plane. In the first step, the complex plane is triangulated, and GRPF searches for the edges of the mesh whose nodes belong to the opposite quadrants of the considered-function values. These edges are called candidate edges. Then, if such an edge is found, the mesh resolution is increased in the region around it, and the number of quadrant changes is computed. Each change of the quadrants by four means that the phase changes by 2π. Each increase of the phase by 2π in the counterclockwise direction means that the root exists around the candidate edge. If the root is detected inside the unit disc, then the considered system is unstable.

The operation principle of GRPF is demonstrated in Fig. 1, where the quadrants of the phase are presented for the function $h(w) = (w-1)(w+1)^2/(w-j)/(w+j)^3$. For this function, the first-order zero is visible in $w = 1$ as the change of phase between quadrants $Q_1 \to Q_2 \to Q_3 \to Q_4$ in the counterclockwise direction on the complex w-plane (i.e., colours ■ → ■ → ■ → ■ change in the counterclockwise direction around $w = 1$). Then, the second-order zero is visible in $w = -1$ as the change of phase between quadrants $Q_1 \to Q_2 \to Q_3 \to Q_4 \to Q_1 \to Q_2 \to Q_3 \to Q_4$ in the counterclockwise direction on the complex w-plane (i.e., colours ■ → ■ → ■ → ■ → ■ → ■ → ■ → ■ change in the counterclockwise direction around $w = -1$). Next, the first-order pole is visible in $w = j$ as the change of phase between quadrants $Q_1 \to Q_2 \to Q_3 \to Q_4$ in the clockwise direction on the complex w-plane (i.e., colours ■ → ■ → ■ → ■ change in the clockwise direction around $w = j$). Finally, the third-order pole is visible in $w = -j$ as the change of phase between quadrants $Q_1 \to Q_2 \to Q_3 \to Q_4 \to Q_1 \to Q_2 \to Q_3 \to Q_4 \to Q_1 \to Q_2 \to Q_3 \to Q_4$ in the clockwise direction on the complex w-plane (i.e., colours ■ → ■ → ■ → ■ → ■ → ■ → ■ → ■ → ■ → ■ → ■ → ■ → ■ change in the clockwise direction around $w = -j$).

Remark. GRPF can naturally be used for meromorphic functions [18], but it is also able to find *FO roots* of the type $(w - w_0)^\alpha$, where $0.5 < \alpha < 1$. Because GRPF verifies the existence of a root based on a phase change between the quadrants on the complex plane, it is able to find *FO roots* as long as the phase change across a branch cut [19] on the complex w-plane is less than $\pi/2$. If this change is greater than $\pi/2$, GRPF is divergent because it tries to refine the mesh in the branch-cut region, which does not lead to a reduction in the phase change. Multiplying the considered function numerous times by itself, which can reduce the phase change across the branch cut and ensure the convergence of GRPF, can be the solution to the problem. This approach increases the order of roots, but does not change their location on the complex plane.

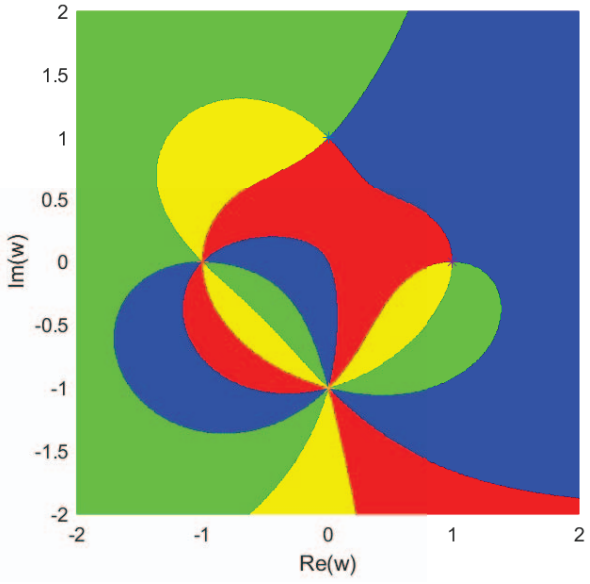

Fig. 1. Quadrants of phase (■ Q_1, ■ Q_2, ■ Q_3, ■ Q_4) for function $h(w) = (w-1)(w+1)^2/(w-j)/(w+j)^3$.

D. Numerical Test of Stability

The proposed numerical test of stability is executed in the following steps:

- the right half-plane is mapped into the unit disc
- GRPF searches for roots of the transformed characteristic equation (11) within the unit disc
- if any root is found within the unit disc, then the analog circuit is unstable.

Remark. The proposed numerical test, like any computations, provides information about the stability of the considered circuit for the assumed accuracy of computations.

III. Exemplary Analog Circuit Analysis

In [10], the FO LC circuit with memristor is considered as in Fig. 2. It includes the FO inductor and capacitor which are respectively described by the following formulas:

$$v_L = L_q D_t^q i_L \tag{13}$$

$$i_C = C_q D_t^q v_C. \tag{14}$$

In (13)–(14), L_q and C_q are, respectively, the fractional inductance and capacitance. One should note that the respective units are given as $[L_q] = H/s^{1-q}$ and $[C_q] = F/s^{1-q}$, refer to [20]. The memristor is described by the following equations:

$$v_M = R(u) i_M \tag{15}$$

$$\dot{u} = f(u, i_M). \tag{16}$$

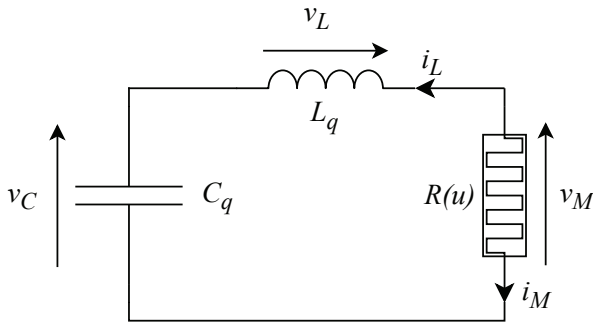

Fig. 2. FO LC circuit with memristor.

In (15)–(16), $R(u)$ is the memristance, $f(u, i_M)$ is the internal-state function and u denotes the internal-state variable. In the circuit considered in [10], the memristance and the internal-state function are respectively taken as follows:

$$R(u) = \frac{3}{2}(u^2 - 1) \tag{17}$$

$$f(u, i_M) = i_M - \frac{3}{5}u - i_M u. \tag{18}$$

For the circuit in Fig. 1, additional two equations can be formulated based on Kirchhoff's circuit laws

$$i_M = -i_L \tag{19}$$

$$v_M = v_L + v_C. \tag{20}$$

Hence, by reducing the number of variables in the system of equations (13)–(20), one obtains

$$\begin{cases} D_t^q x = \frac{1}{C_q} y \\ D_t^q y = -\frac{3}{2L_q}(z^2 - 1)y - \frac{1}{L_q} x \\ D_t^q z = -y - \frac{3}{5} z + yz \end{cases} \tag{21}$$

where $x = v_C$, $y = i_L$ and $z = u$. Let us define the state vector $\mathbf{x} = [x\, y\, z]^\intercal$, which allows one to write (21) in the following compact form:

$$D_t^q \mathbf{x} = \mathbf{f}(\mathbf{x}). \tag{22}$$

Then, let us linearise (21) in the equilibrium point $\mathbf{x}_{eq} = [0\,0\,0]^\intercal = \mathbf{0}$. Hence, we can write the linear approximation to (22) in the equilibrium point

$$D_t^q \mathbf{x} = \mathbf{J}_q \mathbf{x} \tag{23}$$

where

$$\mathbf{J}_q = \left(\frac{\partial \mathbf{f}}{\partial \mathbf{x}} \right)_{\mathbf{x}=\mathbf{x}_{eq}=\mathbf{0}} = \begin{bmatrix} 0 & \frac{1}{C_q} & 0 \\ -\frac{1}{L_q} & \frac{3}{2L_q} & 0 \\ 0 & -1 & -\frac{3}{5} \end{bmatrix} \tag{24}$$

is the Jacobian matrix of $\mathbf{f}$ in the equilibrium point $\mathbf{x}_{eq}$, which depends upon the order of differentiation q due to the parameters L_q and C_q. Applying the Laplace transformation to (23), one obtains the matrix equation

$$s^q \mathbf{x} = \mathbf{J}_q \mathbf{x} + s^{q-1} \mathbf{x}_0. \tag{25}$$

Its characteristic equation is given by

$$\det(s^q \mathbf{I} - \mathbf{J}_q) = 0. \tag{26}$$

Using the bilinear transformation (12), one can detect any unstable root of (26) making use of the GRPF algorithm inside the unit disc $|w| < 1$. That is, the GRPF algorithm searches for the roots of the equation

$$g(w) = \det \left[\left(\frac{1-w}{1+w} \right)^q \mathbf{I} - \mathbf{J}_q \right] = 0. \tag{27}$$

In order to avoid singularity around $w = -1$, we write (27) in the form

$$g(w) = \det \left[(1-w)^q \mathbf{I} - (1+w)^q \mathbf{J}_q \right] = 0 \tag{28}$$

and analyze this characteristic equation further.

Remark. We use the GRPF algorithm for the function which is not an entire function, i.e., it is not holomorphic [21] in the entire complex plane. We actually use the algorithm for the function which is not even meromorphic. We should observe, however, that in the case of the map being the left-hand side of the equation (26), the domain contains the entire complex right half-plane, so the transformed map

$$w \mapsto \det \left[\left(\frac{1-w}{1+w} \right)^q \mathbf{I} - \mathbf{J}_q \right] \tag{29}$$

(refer to (28)) is a holomorphic map in the entire open unit disc $|w| < 1$. It means that GRPF can be applied to the considered case, even if the function is not meromorphic.

Let us take $L_q = 3H/s^{1-q}$ and $C_q = 1F/s^{1-q}$ as in [10]. Then, the circuit is unstable when $q > 0.715$, according to the classical stability test for commensurate FO systems (Theorem II.2 [15]). Let us investigate it numerically with the use of GRPF.

Remark. Of course, one could refer to Theorem II.2 rather than Theorem II.3 and search for zeroes of the rational map yielded by the conformal map transformation $z \mapsto \det(z\mathbf{I} - \mathbf{J}_q)$, where $z = s^q$. This would require checking if the zeroes are located within the cone $|\arg(\mathrm{spec}(\mathbf{J}_q))| < q\pi/2$. However, the considered example allows us to verify the correctness of the proposed stability test, based on GRPF, against the reference stability test for commensurate FO systems (Theorem II.2 [15]).

In Fig. 3, the results of the stability test are presented for $q = 0.5$. The roots are visible as changes of phase between quadrants $Q_1 \to Q_2 \to Q_3 \to Q_4$ in the counterclockwise direction on the complex w-plane (i.e., colours ■ → ■ → ■ → ■ change in the counterclockwise direction around the considered point). The algorithm detects two conjugated roots: $s_1 = 1.28 - j0.749$ and $s_2 = 1.28 + j0.749$, whose absolute value is equal to 1.483. This means that the system is stable as predicted by the classical stability test for commensurate FO systems.

In Fig. 4, the results of the stability test are presented for $q = 0.714$. The algorithm detects two conjugated roots: $s_1 = 0.648 - j0.764$ and $s_2 = 0.648 + j0.764$, whose absolute

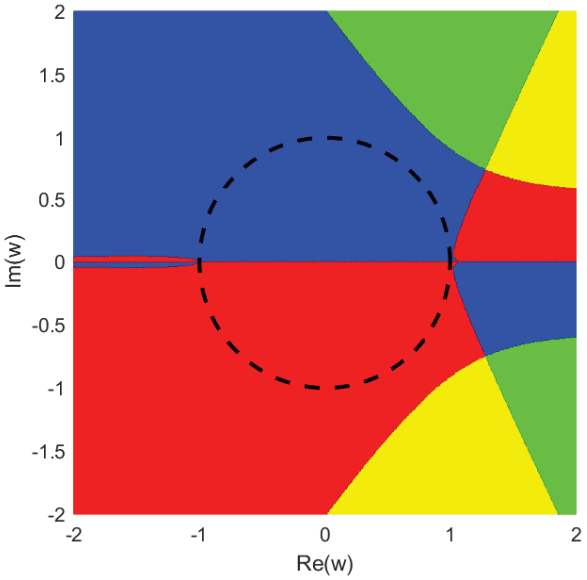

Fig. 3. Quadrants of phase (■ Q_1, ■ Q_2, ■ Q_3, ■ Q_4) for function $g(w)$ when $q = 0.5$. Unit circle is denoted by - -.

value is equal to 1.002. This means that the system is stable as predicted by the classical stability test for commensurate FO systems. For $q = 0.716$, one obtains a very similar graph

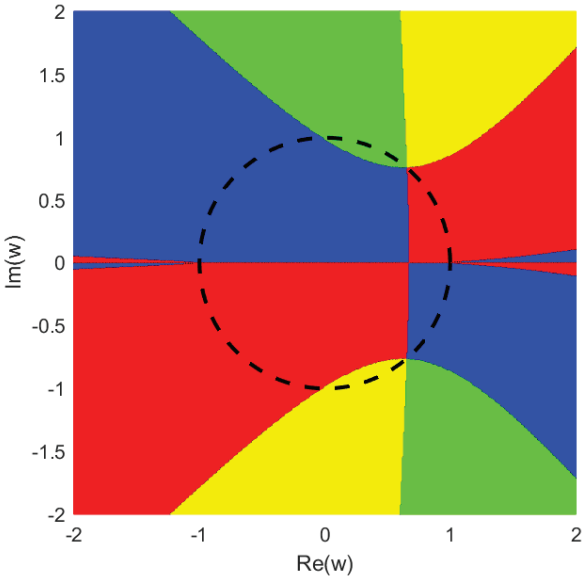

Fig. 4. Quadrants of phase (■ Q_1, ■ Q_2, ■ Q_3, ■ Q_4) for function $g(w)$ when $q = 0.714$. Unit circle is denoted by - -.

of phase quadrants to the one in Fig. 4. However, the algorithm detects two conjugated roots: $s_1 = 0.644 - j0.763$ and $s_2 = 0.644 + j0.763$, whose absolute value is equal to 0.998. This means that the system is unstable as predicted by the classical stability test for commensurate FO systems. It is worth noting that a slight change of parameter q from 0.714 to 0.716 is precisely detected by GRPF.

In Fig. 5, the results of the stability test are presented for $q = 0.99$. The algorithm detects two conjugated roots: $s_1 = 0.369 - j0.573$ and $s_2 = 0.369 + j0.573$, whose absolute value is equal to 0.682. This means that the system is unstable as predicted by the classical stability test for commensurate FO systems.

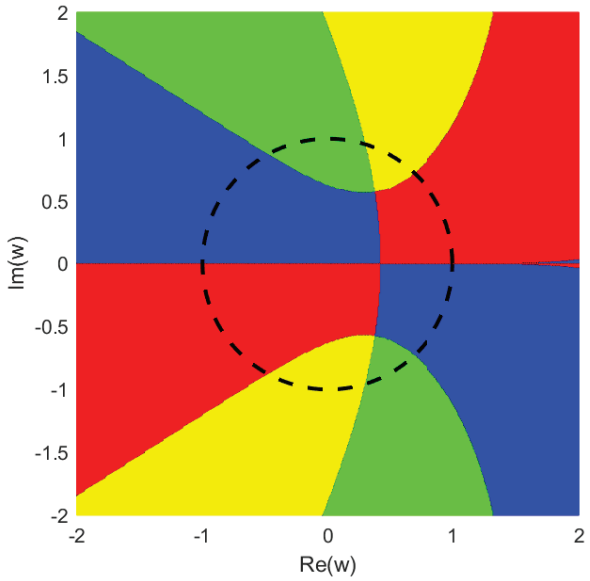

Fig. 5. Quadrants of phase (■ Q_1, ■ Q_2, ■ Q_3, ■ Q_4) for function $g(w)$ when $q = 0.99$. Unit circle is denoted by - -.

To sum up, the proposed test correctly detects parameter ranges of either stability ($q < 715$) or instability ($q > 0.715$) for the considered analog circuit, proving the efficiency and generality of our stability test.

IV. Conclusion

In this contribution, we present complex-plane mapping of the instability region into the unit disc, and the efficient numerical method (GRPF) for root detection in this region. It allows one to detect the instabilities of analog circuits whose characteristic equations do not have to be polynomials. In order to demonstrate the applicability of our stability test, the memristor-based chaotic circuit is analyzed, whose stability depends on the value of the FO parameter. The proposed test correctly detects circuit instabilities, confirming its efficiency and generality.

Source Code

The source code for GRPF can be found at: https://github.com/PioKow/GRPF, and it is licensed under the MIT License.

REFERENCES

[1] G. Chen, *Stability of Nonlinear Systems*. John Wiley & Sons, Ltd, 2005.

[2] J. Osiowski and J. Szabatin, *Fundamentals of Circuit Theory III (in Polish)*. Warsaw: Wydawnictwo WNT, 1995.

[3] A. Suarez, "Check the stability: Stability analysis methods for microwave circuits," *IEEE Microw. Mag.*, vol. 16, no. 5, pp. 69–90, 2015.

[4] The MathWorks Inc., "Matlab version: 9.10.0 (r2021a)," Natick, Massachusetts, United States, 2021. [Online]. Available: https://www.mathworks.com

[5] C. Hwang and Y.-C. Cheng, "A numerical algorithm for stability testing of fractional delay systems," *Automatica*, vol. 42, no. 5, pp. 825–831, 2006.

[6] J. Sabatier, C. Farges, and J.-C. Trigeassou, "A stability test for non-commensurate fractional order systems," *Syst. Control Lett.*, vol. 62, no. 9, pp. 739–746, 2013.

[7] Ł. Grzymkowski, D. Trofimowicz, and T. P. Stefański, "Stability analysis of interconnected discrete-time fractional-order lti state-space systems," *Int. J. Appl. Math. Comput. Sci.*, vol. 30, no. 4, pp. 649–658, 2020.

[8] D. Trofimowicz and T. P. Stefański, "Testing stability of digital filters using optimization methods with phase analysis," *Energies*, vol. 14, no. 5, p. 1488, 2021.

[9] P. Kowalczyk, "Global complex roots and poles finding algorithm based on phase analysis for propagation and radiation problems," *IEEE Trans. Antennas Propag.*, vol. 66, no. 12, pp. 7198–7205, 2018.

[10] D. Cafagna and G. Grassi, "On the simplest fractional-order memristor-based chaotic system," *Nonlinear Dyn.*, vol. 70, no. 2, pp. 1185–1197, 2012.

[11] J. Gulgowski, T. P. Stefański, and D. Trofimowicz, "On applications of fractional derivatives in circuit theory," in *2020 27th International Conference on Mixed Design of Integrated Circuits and System (MIXDES)*, 2020, pp. 160–163.

[12] J. Gulgowski, T. P. Stefański, and D. Trofimowicz, "On applications of elements modelled by fractional derivatives in circuit theory," *Energies*, vol. 13, no. 21, 2020.

[13] E. Ahmed, A. El-Sayed, and H. El-Saka, "Equilibrium points, stability and numerical solutions of fractional-order predator-prey and rabies models," *J. Math. Anal. Appl.*, vol. 325, no. 1, pp. 542–553, 2007.

[14] H. Delavari, D. Baleanu, and J. Sadati, "Stability analysis of Caputo fractional-order nonlinear systems revisited," *Nonlinear Dyn.*, vol. 67, no. 4, pp. 2433–2439, 2012.

[15] D. Matignon, "Stability results for fractional differential equations with applications to control processing," in *CESA'96 IMACS Multiconference: computational engineering in systems applications*, 1996, pp. 963–968.

[16] E. W. Weisstein, "Argument principle," *From MathWorld–A Wolfram Web Resource*, 2023. [Online]. Available: https://mathworld.wolfram.com/ArgumentPrinciple.html

[17] ——, "Delaunay triangulation," *From MathWorld–A Wolfram Web Resource*, 2023. [Online]. Available: https://mathworld.wolfram.com/DelaunayTriangulation.html

[18] ——, "Meromorphic function," *From MathWorld–A Wolfram Web Resource*, 2023. [Online]. Available: https://mathworld.wolfram.com/MeromorphicFunction.html

[19] ——, "Branch cut," *From MathWorld–A Wolfram Web Resource*, 2023. [Online]. Available: https://mathworld.wolfram.com/BranchCut.html

[20] T. P. Stefański and J. Gulgowski, "Electromagnetic-based derivation of fractional-order circuit theory," *Commun. Nonlinear Sci. Numer. Simul.*, vol. 79, p. 104897, 2019.

[21] E. W. Weisstein, "Holomorphic function," *From MathWorld–A Wolfram Web Resource*, 2023. [Online]. Available: https://mathworld.wolfram.com/HolomorphicFunction.html